CFD Modelling of flows in a large stormwater detention and settling basin

Modélisation numérique 3D des écoulements dans un bassin de retenue-décantation des eaux pluviales de grande taille

Gislain Lipeme Kouyi[1], Luis Arias[1], Sylvie Barraud[2], Jean-Luc Bertrand-Krajewski[1]

[1]: Université de Lyon, F-69000, Lyon, France
INSA-Lyon, LGCIE, F- 69621 Villeurbanne, France
{gislain.lipeme-kouyi, jean-luc.bertrand-krajewski}@insa-lyon.fr,
luisariasz@gmail.com

[2]: Université de Lyon, F-69000, Lyon, France
Université Lyon 1, LGCIE, F-69622, Villeurbanne, France
INSA-Lyon, LGCIE, F-69621, Villeurbanne, France
sylvie.barraud@insa-lyon.fr

RÉSUMÉ

Un modèle 3D du bassin de retenue-décantation de grande taille de l'OTHU (Observatoire de Terrain en Hydrologie Urbaine - **www.othu.org**), situé à Chassieu (Rhône, France) a été élaboré. Les écoulements turbulents à surface libre ont été modélisés à l'aide du logiciel commercial CFD Ansys Fluent v.12. Cette approche de modélisation a été comparée aux observations in situ en ce qui concerne les zones préférentielles de dépôt. Ces zones correspondent surtout aux zones proches du fond au niveau desquelles l'énergie cinétique turbulente est faible (de l'ordre de 10^{-5} m^2/s^2). Ainsi, une approche fondée sur le seuillage de l'énergie cinétique turbulente, estimée à l'aide du modèle RSM (Reynolds Stress Model), permet de représenter correctement les zones de dépôt dans des ouvrages réels de grande taille et par conséquent une forte probabilité de reproduire l'efficacité de traitement.

ABSTRACT

A 3D model of the OTHU (Field observatory in urban hydrology - **www.othu.org**) large detention and settling basin was developed, aiming to produce more realistic and transferable results. The free surface turbulent flow was simulated by means of the CFD commercial software Ansys Fluent 12, which solves the Reynolds equations by using the finite volume method. This approach was compared to in situ observations of the preferential settling zones. The settling zones correspond primarily to low (around 10^{-5} m^2/s^2) turbulent kinetic energy zones (estimated by the RSM turbulent model). An approach based on a turbulent kinetic energy threshold computed by means of the RSM model allows the settling zones to be correctly represented in a large real settling basin. Therefore there is a high potential to assess the efficiency of the basin.

KEYWORDS

CFD modelling, hydrodynamics, settling basin, stormwater, turbulent kinetic energy

1 INTRODUCTION

Stormwater detention basins were initially built to reduce flood risks. However, high pollutant removal rates due to the settling of particles were observed by many authors (e.g. Marsalek et al., 1992; Stovin, 1996 ; Ta, 1999; Strecker et al., 2004) in numerous facilities, with the result that detention basins are more and more used as detention and settling facilities.

Adamsson et al. (2003), Dufresne et al. (2008) and other authors in the last fifteen years carried out research programs on small scale physical models to understand and model settling processes. However, the good results obtained and published in the literature remain difficult to apply to full size stormwater basins because of (i) the variability and heterogeneity of the particles carried by the turbulent, three-dimensional free surface flows in complex geometry basins, (ii) the difficulties to represent settling and re-suspension processes of these particles, and (iii) the distribution of the energy near the bottom of the basin (particularly the turbulent kinetic energy) assumed to strongly influence the settling and re-suspension processes. Consequently, in order to contribute to improving the design and the management of large stormwater detention and settling basins, experimental and modelling investigations have been carried out in the large Django Reinhardt stormwater detention and settling basin in Chassieu (Rhône, France), as one of the research actions of the OTHU (Field Observatory in Urban Hydrology – www.othu.org). The volume and the base area of the Django Reinhardt basin are respectively 32,200 m^3 and 11,302 m^2.

The sustainable techniques and strategies for stormwater management require the improvement of the conception, the design and the management of detention-infiltration basins. This improvement will be based to a large extent on modelling tools. Torres (2008) investigated the experimental and 2D CFD modelling of the hydrodynamics and solid transport in the Django Reinhardt basin. This paper will focus on the 3D CFD modelling of the free surface turbulent flows in the same basin. 3D CFD modelling have already been successfully used under various hydraulic conditions: in combined sewer overflow chambers (e.g. Lipeme Kouyi et al., 2003; Lipeme Kouyi, 2004), in detention and sedimentation tanks (Stovin, 1996; Bartone and Uchrin, 1999; Kowalski et al., 1999; Adamsson et al., 2003; Jayanti and Narayanan, 2004), for the improvement of hydraulic performance in a storm-water clarifier (He et al., 2008), and in hydrodynamic separators (Alkhaddar et al., 2001).

This paper assesses the ability of 3D modelling with Ansys Fluent 12 CFD software to represent the hydrodynamics and to reproduce the settling zones in a large complex stormwater detention and settling basin.

2 MATERIALS AND METHODS

2.1 Experimental site and materials

The Django Reinhardt detention-infiltration facility was built in 1975 in Chassieu (Rhône, France) in order to collect stormwater from a 185 ha industrial catchment. It was rehabilitated (to remove surface clogging) in 1985, in 2002 and then further retrofitted in 2004. The facility is composed of two sub-basins connected with a 60 cm diameter pipe. The first one is a detention and settling basin (Figure 1) where the stormwater is stored before being released downstream to the infiltration sub-basin. During dry weather, the settling basin receives a small amount of water from the surrounding industries, which are only authorized to discharge (theoretically) unpolluted cooling waters. The bottom of the settling basin is sealed with bitumen and is equipped with a low-flow trapezoidal channel collecting and guiding the dry weather flow towards three outlets. The sides of the settling basin are covered with a plastic liner.

Stormwater enters the settling basin via two 1.6 m circular pipes (labelled as inlet 1 and inlet 2 in Figure 1). In order to improve the settling process, a 1 m high detention wall was built in 2004. There are three 19 cm diameter outlet orifices (labelled o1, o2 and o3 in Figure 1) in the detention wall. When the water level is higher than the detention wall, an overflow weir is used as an additional outlet. The stormwater outflow towards the infiltration sub-basin is limited to 350 L/s by a regulator (Hydroslide® gate).

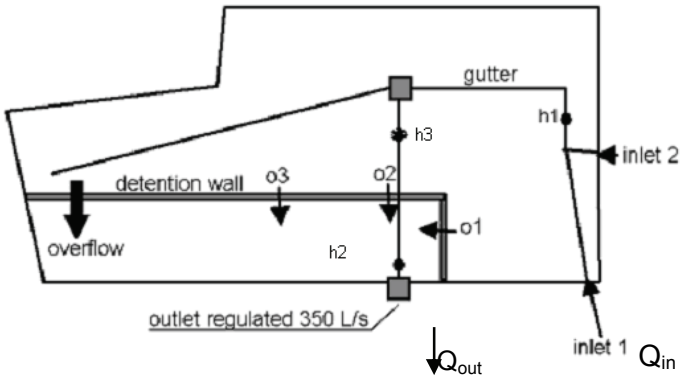

Q_{out}:outlet flow rate (towards infiltration basin)

Q_{in}: inlet flow rate

o1: orifice no.1

o2: orifice no.2

o3: orifice no.3

h1 : water depth sensor no.1

h2 : water depth sensor no.2

h3 : water depth sensor no.3

: low-flow sedimentation pit

Figure 1: Scheme of the Django Reinhardt detention and settling basin after its retrofit in 2004 (Bardin and Barraud, 2004)

The inlet and outlet discharges are calculated from simultaneous measurements of water depth and velocity in the pipes. Three water depth sensors are located on the bottom of the basin (labelled h1, h2 and h3 in Figure 1). All variables are recorded with a 2 minute time step to a S50 Sofrel data logger.

Twelve sediment traps installed on the bottom of the basin collect settled sediments during storm events (Figure 2). Each trap is composed of two assembled plastic boxes with an internal honeycomb structure to prevent the scouring of trapped sediments. The location of the 12 traps was chosen using, on one hand, previous observations of sedimentation zones and, on the other, some hydrodynamic modelling results showing flow velocities in recirculation zones (Torres, 2008).

The traps are numbered according to their altitude, from 1 (lowest) to 12 (highest). After a storm event, samples made up of a mixture of water and sediment are transported as quickly as possible to the laboratory, where settling velocity and particle-size distributions are measured according to the VICAS protocol (Gromaire and Chebbo, 2003) and Laser Particle Sizer (LPS) technique, respectively.

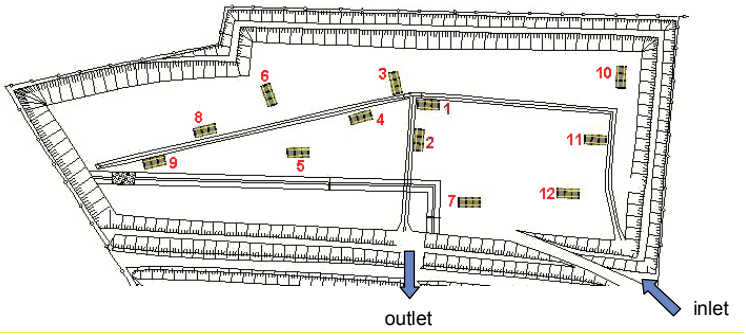

Figure 2: Sediment traps location and sampling devices (top view), (TORRES, 2008)

2.2 Modelling of flows and distribution of particles on the bed of the basin

3D steady state simulations were carried out with the software CFD Ansys Fluent v.12 in order to further understand the hydrodynamic behaviour and the settling zones by means of the turbulent kinetic energy threshold computed from the Reynolds constraints. One of the aims of this study was to test a complete hydrodynamic model based on the computation of Reynolds stress, taking into account the heterogeneity and the anisotropy of the turbulence. Second order schemes for all terms of the main equations (flow, Volume Of Fluid model for the computation of free surface and Reynolds Stress Model - RSM - for turbulence) were used to simulate the hydraulic operation of the Django-Reinhardt basin. We test whether settling areas were correlated to low bed shear and Reynolds stresses as demonstrated by Adamsson et al. (2003) or Terfous et al. (2006).

2.2.1 Equations of motion and formulation of the problem

Partial derivative equations describing the flow (Reynolds equations) are written in a conservative form, to establish relations between the pressure, velocities and Reynolds stress (Versteeg and Malalasekera, 1995). The form of partial derivative equations for biphasic application is as follows:

- The continuity equation for each phase which is called *q*:

$$\begin{cases} \dfrac{\partial \alpha_q}{\partial t} + U_i \dfrac{\partial \alpha_q}{\partial x_i} = 0 \\ 0 \le \alpha_q \le 1 \\ \sum_{q=1}^{n} \alpha_q = 1 \end{cases} \qquad (1)$$

where *n* is the number of phases, U_i the mean velocity components and α_q is the volume fraction of phase *q*. In each cell, the overall volume mass ρ and viscosity μ are computed using the volume fraction as follows:

$$\begin{cases} \rho = \sum_{q=1}^{n} \alpha_q \rho_q \\ \mu = \sum_{q=1}^{n} \alpha_q \mu_q \end{cases} \qquad (2)$$

- The momentum equation :

$$\frac{\partial \rho U_i}{\partial t} + U_i \frac{\partial \rho U_i}{\partial x_i} = -\frac{\partial P}{\partial x_i} + \rho g_i + \mu \frac{\partial^2 U_i}{\partial x_j \partial x_j} - \frac{\partial \rho \left(\overline{u_i' u_j'} \right)}{\partial x_j} \qquad (3)$$

where *P* is the pressure term and *g* is the gravitational acceleration. Equation (3) represents the Reynolds Averaged Navier-Stokes (RANS) equations system (for *i* and *j* equal to 1, 2 and 3). The terms $\rho \overline{u_i' u_j'}$ called Reynolds tensors can be estimated by means of closing equations such as in the RSM turbulence model.

This software uses the finite volume method for solving the partial derivative equations presented above. Therefore the computational meshes should be built as volumes of control

2.2.2 Boundary conditions

Several kinds of boundary conditions are proposed in the CFD code, such as symmetry, inlet and outlet pressure, imposed velocity, etc. Three of those conditions are used for our study: inlet velocity, outlet pressure and roughness for the assessment of the wall functions.

The first boundary condition – inlet velocity - is an imposed value of the velocity. The flow is thus injected through a wet section to obtain the expected inlet flow rate. In this case, the length of the inlet pipe must be sufficient to enable the velocity profile to be developed. The length required is 5 to 10 times the water depth at the inlet boundary. The second condition – outlet pressure - is applied at the outlets or for the free surface modelling by setting the atmospheric pressure value. The roughness condition is used to account for the boundary layer near the wall.

The value of the water volume fraction is imposed and is equal to 1 in the water and equal to 0 in the air. The computation of the turbulent intensity *I* and the hydraulic diameter D_h enables us to obtain the inlet boundary values for turbulence:

$$I = 0.16 R_e^{-1/8} \text{ with } R_e = \frac{UD_h}{\nu} \text{ the Reynolds number} \quad (4)$$

2.2.3 Computational mesh

To obtain correct modelling results, we built the mesh grid with a lot of detail because the more meshes we have, the more accurate the results are. However the computation time increases dramatically with the level of detail (e.g. for the calculation of 25,000 iterations with 500,000 computational cells, the current computation time can reach 2 days with a PC 64-bit under Linux). So we tried to find a balance between quality of results and computation time, and we chose to proceed with 720,000 computational cells (see Figure 3).

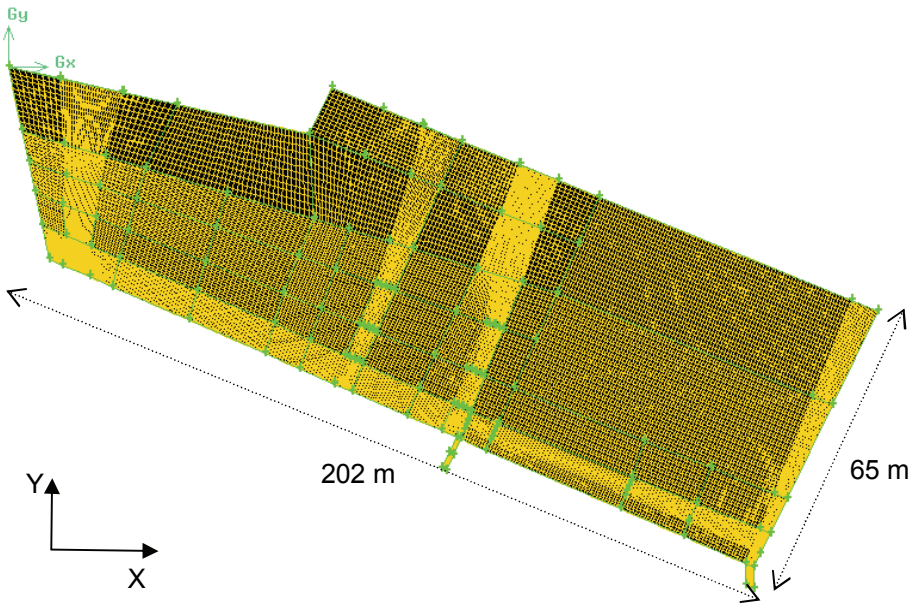

Figure 3: Computational hexahedral mesh of the basin for 3D simulations

3 RESULTS AND DISCUSSION

3.1 3D modelling of velocity field

We simulated flows in the basin for several inlet flow rates. We checked mainly two configurations, one with the computation of the free surface by means of VOF (Volume Of Fluid) models and another without free surface (a smooth wall was imposed on the top of the basin). The VOF model has been successfully tested and validated by Lipeme Kouyi et al. (2003) and others in several hydraulic conditions (e.g. Mueller et al., 2007). Both k-ε and RSM turbulence models were used. The simulations were done with "averaged" stationary consideration. The results, displayed in Figure 4, show the presence of large vortices. This structure of velocity field had already been identified by Torres (2008) when using the Barré de Saint Venant-based CFD Rubar 20 Code. The velocity field can give us an idea of the settling zones.

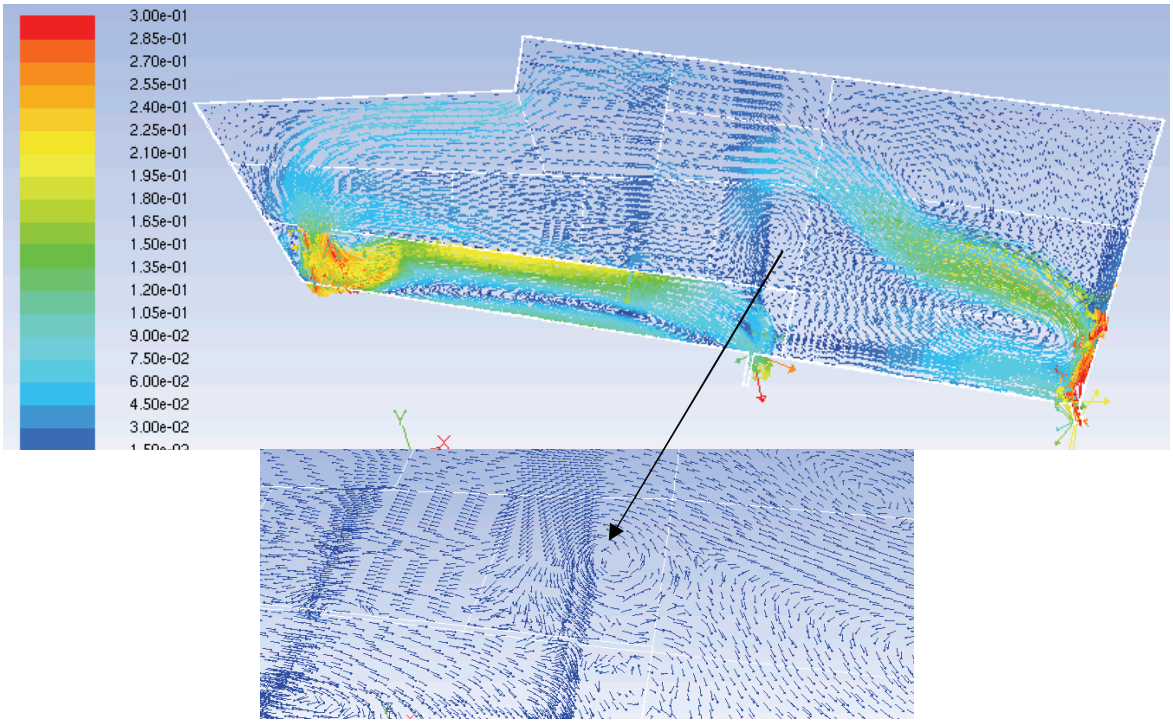

Figure 4: Free surface velocity field for the inlet flow rate of 0.3 m^3/s and with the k-ε turbulent model

3.2 Assessment of the sediment distribution at the bottom

We tested two configurations in "averaged" stationary regime: a full basin with only water without the modelling of the free surface (considering a smooth wall at the top of the basin), and a basin with free surface. We then quantified the following parameters near the bottom in order to identify their influence on the location of settling zones: shear stress, coefficient of friction and turbulent kinetic energy.

Several inlet flow rates (labelled Q_{inlet} in the following figures) were injected into the two configurations (0.1 m^3/s, 0.3 m^3/s, 1 m^3/s, 1.5 m^3/s ...). We also tested two types of turbulence models: the k-ε and RSM turbulent models. The objective was to see the effect of anisotropy on the energy distribution near the bottom.

3.2.1 Results with the RSM model and without the free surface

The figure 5 shows areas where the coefficient of friction is low. This coefficient represents the ratio between the shear stress and the dynamic pressure.

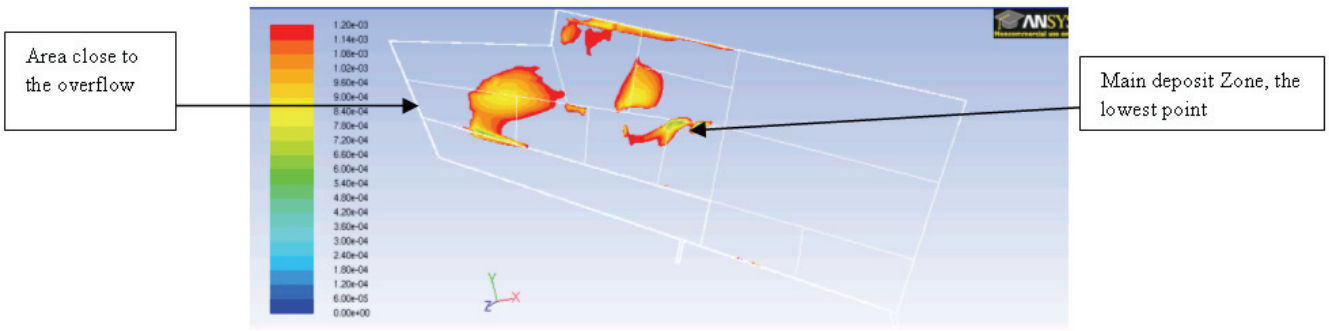

Figure 5: Areas corresponding to a friction coefficient <0.0012 – Q_{inlet} = 1m^3/s

Concerning the influence of shear stress on the settling processes, Adamsson et al. (2003) showed that in the case of a flow composed of a large asymmetric recirculation, particles would deposit in areas of low shear stresses (0.03 - 0.04 Pa). Figure 6 shows the areas obtained for low shear stresses. However we found that this graph did not represent adequately the deposit zones in the real basin.

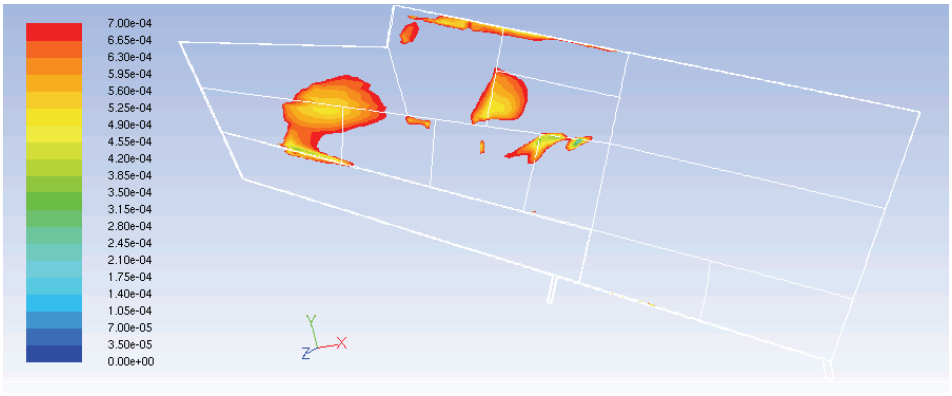

Figure 6: Areas corresponding to a shear stress <0.0007Pa

On the other hand, when plotting the areas with lower values of turbulent kinetic energy, it was possible to adequately represent the settling zones of the real basin as shown in Figure 7. The analysis of these results enabled us to establish a threshold of0.00002 m^2/s^2: Particles settle in areas close to the bottom where the turbulent kinetic energy is below this threshold.

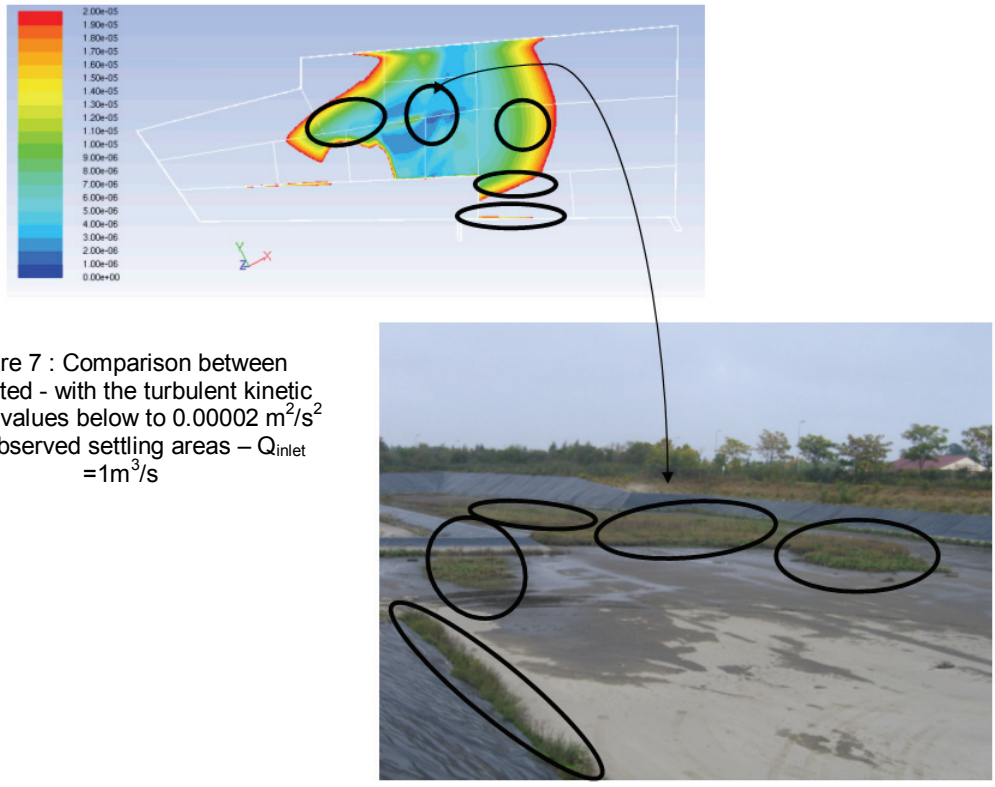

Figure 7 : Comparison between simulated - with the turbulent kinetic energy values below to 0.00002 m^2/s^2 and observed settling areas – Q_{inlet} =1m^3/s

3.2.2 Results with the model k-ε and without the free surface

The convergence was faster with this turbulent model. We found that the settling zones were areas where the turbulent kinetic energy was less than 0.00015 m^2/s^2. The results are shown in Figure 8.

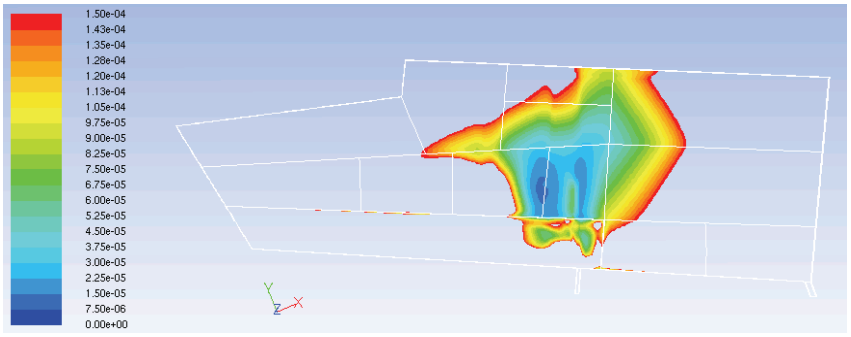

Figure 8: Areas corresponding to a turbulent kinetic energy < 0.00015 m^2/s^2 - Q_{inlet} =1m^3/s

So the value of the turbulent kinetic energy threshold depends of the turbulent model.

3.2.3 Results accounting for the free surface in the basin with the k-ε model

The shear stresses and the friction coefficient were estimated near the bottom of the basin. The settling zones indicated by this approach show good agreement with observed zones (Figure 9). The results highlight as well the sedimentation zone located in front of the orifice o1 (Figures 9 and 10).

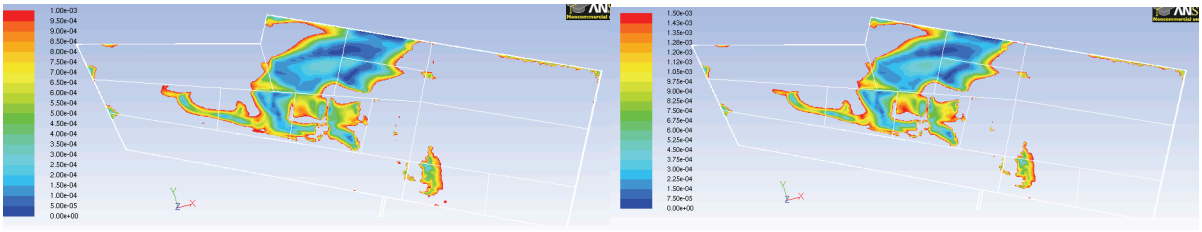

Figure 9: Areas corresponding to: a) shear stress values <0.001 pa, b) friction coefficient <0.0015

Taking into account the free surface improves the representation of settling zones by using the shear stress and the friction coefficient.

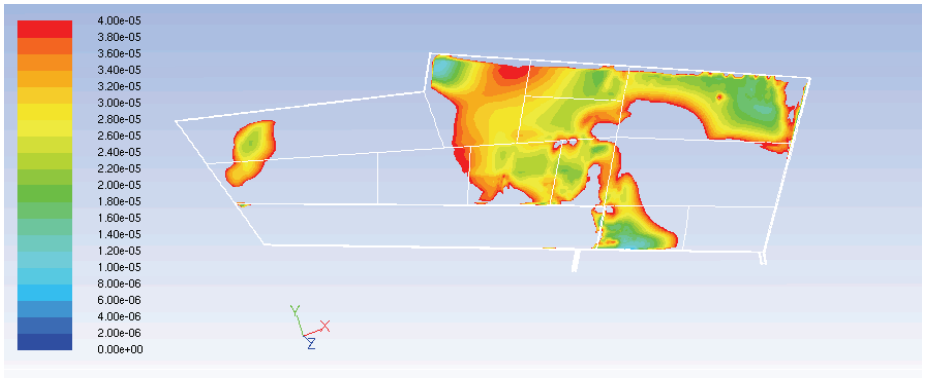

Figure 10: Areas corresponding to a turbulent kinetic energy <0.00004 m^2/s^2.

The representation of the settling zones derived from the use of the threshold of turbulent kinetic energy (Figure 10) corresponds to the observed zones indicated in Figure 7. The settling zone located in front of orifice 1 is well represented when the free surface is taken into account.

3.3 Summary of results

The results showed that in a large detention basin, the computation of a threshold for the shear stress and the coefficient of friction could represent settling areas adequately only in the case of a model taking into account the free surface. In contrast, when using a threshold of turbulent kinetic energy, modelled by RSM or k-ε, the settling zones were closer to reality, but that there is a difference in the threshold values..

It was also shown that the computation of velocity fields of the free surface could give an idea of areas

of preferential settling areas.

Taking into account the free surface improves the representation of the settling zone (see figure 7). Indeed, the free surface influences strongly the pressure field and therefore the shear stress values. That's why the threshold values are different with and without free surface modelling.

The central settling zone was found to be the area with the highest amount of sediments. The approach based on the threshold of turbulent kinetic energy enables to represent this zone. For the storm event of June 26th 2009 for example, particle size analysis were performed on samples collected from four traps (traps 1, 2, 3 and 7). We achieved an average diameter (D_{50}) of 115 µm for trap 1, 110 µm for trap 2, 117 µm for trap 3 and 56 µm for trap 7. In this central zone the particles have high diameters and the thickness of the sediment layer is important (See figure 11).

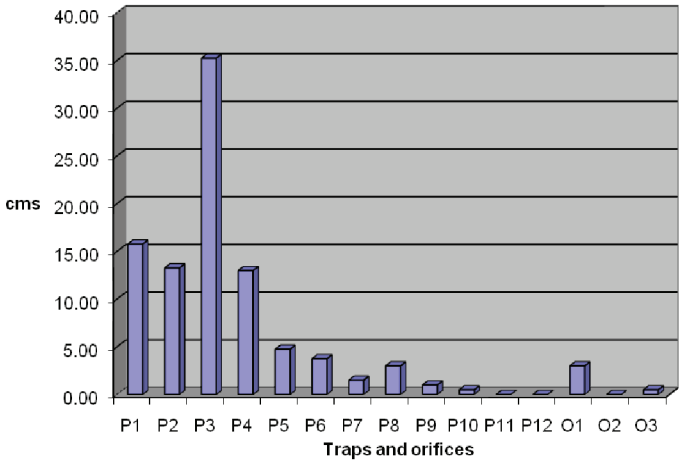

Figure 11: Thickness of sediment layer at sediment traps and in front of orifices – observed in July 2009

4 CONCLUSIONS

In order to improve the design and the management of large stormwater detention and settling basins, modelling investigations have been carried out in the Django Reinhardt basin in Chassieu (Rhône, France). Three-dimensional modelling of hydrodynamics was carried out with the Ansys Fluent v.12 CFD software in order to further understand the hydraulics and to reproduce the preferential settling zones by means of the turbulent kinetic energy threshold arising from the Reynolds constraints modelling. The results of the simulations showed the ability of the 3D model to represent the observed settling zones according to the vortices in velocity fields.

The approach based on the computation of the flows with the RSM turbulent model and the threshold of the turbulent kinetic energy enabled us to understand the hydrodynamic behaviour and the settling processes of the basin. The threshold values were $2x10^{-5}$ m^2/s^2 in case of a basin model without the free surface and $4x10^{-5}$ m^2/s^2 in case of a basin accounting for the free surface flows. The modelling of the free surface has an important role in the settling processes. Consequently, CFD modelling may help to obtain thresholds of the turbulent kinetic energy near the bed of complex facilities in order to improve the modelling of the settling processes. For the management of large stormwater basins, simplified models could be elaborated using the CFD approach which would be more appropriate for practitioners.

AKNOWLEDGEMENTS

The authors thank the OTHU (Field Observatory in Urban Hydrology) for scientific support and for financing, ANR (Ecopluies Project PRECODD) and DRI (exDRAST) for financing this project.

LIST OF REFERENCES

Adamsson A., Stovin V., Bergdahl L. (2003). *Bed Shear Stress Boundary Condition for storage tank sedimentation*. Journal of Envrionmental Engineering, Vol. 129, No. 7, jul/2003, pages 651–658.

Alkhaddar, R.M., Higgins, P.R., Phipps, D.A., and Andoh, R.Y.G. (2001*). Residence time distribution of a model*

hydrodynamic vortex separator." Urban Water, Vol.3, pages. 17-24.

Bartone D., Uchrin C. (1999). *Comparison of pollutant removal efficiency for two residential storm water basins* Journal of Environmental Engineering, Vol. 125, No. 7, july/2009, pages 674-677.

Bertrand-Krajewski J.L. (2004). *TSS concentration in sewers estimated from turbidity measurements by means of linear regression accounting for uncertainties in both variables*. Water Science and Technology, Vol. 50, No. 11, pages 81-88.

Dufresne M., Vazquez J., Terfous A., Ghenaim A., Poulet J-B. (2009). *Experimental investigation and CFD modelling of flow, sedimentation, and solids separation in a combined sewer detention tank*. Computer & Fluids, 38, 1042-1049...

Gromaire M.-C., and Chebbo G. (2003). *Mesure de la vitesse de chute des particules en suspension dans les effluents urbains, protocole VICAS, manuel de l'utilisateur*. Rapport, Marne-la-Vallée (France): ENPC CEREVE, novembre 2003, 70 p.

He G., Wood J., Marsalek J., Rochfort Q. (2008). *Using CFD modelling to improve the inlet hydraulics and performance of a storm-water Clarifier. Journal of Environmental Engineering*, Vol. 134, No. 9, sep/2008, pages 722-730.

Jayanti S., and Narayanan S. (2004). *Computational study of particles-eddy interaction in sedimentation tanks.* Journal of Environmental Engineering, Vol. 130, No. 1, pp. 37-49.

Kowalski R., Reuber J., and Kongeter J. (1999). *Investigations into and optimisation of the performance of sewage detention tanks during storm rainfall events*. Water Science and Technology, Vol. 39, No. 2, pp. 43-52.

Lipeme Kouyi G., Vazquez J., and Poulet J-B. (2003). *3D free surface measurement and numerical modelling of flows in storm overflows.* Flow Measurement and Instrumentation, Vol. 14, No. 3, pp. 79-87.

Lipeme Kouyi G. (2004). *Expérimentations et modélisations tridimensionnelles de l'hydrodynamique et de la séparation particulaire dans les déversoirs d'orage.* PhD thesis, EENGEES, Université Louis Pasteur, Strasbourg, 274 pages.

Marsalek J, Watt W., Henry D. (1992). *Retrofitting stormwater ponds for water quality control*. Water Poll Res J.Canada, 27(2), pages 403-422.

Milisic V. (2004). *Analyse du transport des matières en suspension dans les bassins de stockage-décantation de la pollution des surverses des réseaux unitaires. Application à la conception et à la gestion de ces bassins dans la ville de Marseille.* Syntheses and conclusions of PhD thesis of F. Schmitt, 66 pages.

Mueller D. S., Abad J. D., Garcia C. M, Gartner J. W., Garcia M. H., Oberg K.O. (2007). *Errors in acoustic Doppler Profiler Velocity measurements caused by fow disturbance.* Journal of Hydraulic Engineering, Vol. 133, N°12, 1411-1420.

NF EN 27027 (1994). *Qualité de l'eau - Détermination de la turbidité.* Paris (France): AFNOR, avril 1994, 11 p.

Stovin, V. (1996). *The prediction of sediment deposition in storage chambers based on laboratory observations and numerical simulations*. PhD thesis, University of Sheffield.

Strecker E., Quigley M., Urbonas B., Jones J., Clary J., and O'brien J. (2004). Urban stormwater BMP performance: Recent findings from the International Stormwater BMP Database Project. Proceedings of Novatech 2004, Lyon, France, 6-10 Juin, 407-414. ISBN 2-9509337-5-0.

Terfous A., Vazquez J., Lipeme Kouyi G., Dufresne M., Poulet J-B., Ghenaim A., and Vasile C. (2006). Contribution to the 3D modelling of the suspended sediment flow in stormwater tank using Particle Image Velocimetry. Proceedings of the 7th International Conference on Hydroinformatics. Nice, France, 4-8 sept., Edited by P. Gourbesville, J. Cunge, V. Guinot and S.Y. Liong, Research Publishing services,1341-1348, ISBN 81-903170-3-2.

Torres A. (2008). *Décantation des eaux pluviales dans un ouvrage réel de grande taille : éléments de réflexion pour le suivi et la modélisation*. Phd thesis, INSA de Lyon, 368 pages.

Versteeg H., Malalasekera, W. (1995). *An introduction to computational fluid dynamics, the finite volum method*. Prentice Hall, London, UK, 257 p.